Available online at www.sciencedirect.com

ScienceDirect

Transportation Research Procedia 00 (2018) 000–000

Transportation Research Procedia

www.elsevier.com/locate/procedia

International Symposium of Transport Simulation (ISTS'18) and the International Workshop on Traffic Data Collection and its Standardization (IWTDCS'18)

Relationships between macroscopic fundamental diagram hysteresis and network-wide traffic conditions

Amr M. Wahaballa[a,b], Seham Hemdan[b], Fumitaka Kurauchi[b,*]

[a]*Aswan University, Aboelreesh Kebly, Aswan 81542, Egypt*
[b]*Gifu University, 1-1 Yanagido, Gifu-shi, Gifu 501-1193, Japan*

Abstract

The macroscopic fundamental diagram (MFD) is a graph relating an average network flow to the average density and is used to evaluate traffic-control strategies. However, a large urban network may have multiple flows for any given density; such a condition is termed an MFD hysteresis loop. The relationships between this loop and network conditions must be studied when evaluating the effects of traffic-control strategies on network performance, especially for multi-modal networks that have received little attention to date. Here, we investigated relationships between loop width and height, the spatial density distribution, and network performance, via multi-agent simulation of various traffic conditions for cars and buses. We partitioned the MFD loop into two parts (the congestion-building and dissipation periods) and found that the correlations between the density distribution and network performance, and the heights, of the two parts were stronger than the correlations obtained when the overall loop height was used, because the two heights exhibited opposite effects on traffic conditions. We conclude that network performance inversely affects flow reduction when the network is loading, whereas the heterogeneous density distribution increases flow reduction during network unloading (as congestion dissipates). The criteria for loop partitioning that we develop reveal several relationships not yet addressed in the literature, and aid in the evaluation of network performance when MFD hysteresis is in play, facilitating appropriate traffic-control decisions.

© 2018 The Authors. Published by Elsevier Ltd.
This is an open access article under the CC BY-NC-ND license (https://creativecommons.org/licenses/by-nc-nd/4.0/)
"Peer-review under responsibility of the scientific committee of the International Symposium of Transport Simulation (ISTS'18) and the International Workshop on Traffic Data Collection and its Standardization (IWTDCS'18)"

Keywords: Macroscopic fundamental diagram; hysteresis loop; multi-modal network; performance; density distribution

* Corresponding author. Tel.: +81-58-293-2443; fax: +81-58-293-2393.
E-mail address: kurauchi@gifu-u.ac.jp

2352-1465 © 2018 The Authors. Published by Elsevier Ltd.
This is an open access article under the CC BY-NC-ND license (https://creativecommons.org/licenses/by-nc-nd/4.0/)
"Peer-review under responsibility of the scientific committee of the International Symposium of Transport Simulation (ISTS'18) and the International Workshop on Traffic Data Collection and its Standardization (IWTDCS'18)"

1. Introduction

Policy-makers need to evaluate the effects of traffic-control strategies (e.g., road pricing) on network-wide traffic conditions to determine which strategy to implement. The macroscopic fundamental diagram (MFD), which relates the average network flow to the average density, is a simple method by which traffic-control effects can be evaluated. Geroliminis and Daganzo (2008) proved the utility of the MFD using real data from Yokohama city. Since that time, the MFD has been widely employed to evaluate traffic control-effects on transportation network performance (e.g., Knoop et al., 2012, Zheng et al., 2016). Based on empirical data for various freeways, Buisson and Ladier (2009) observed the MFD hysteresis loop, in which a given density has different flow values, and concluded that heterogeneous density spread might explain the loop. Later, based on simulations, Gayah and Daganzo (2011) concluded that an MFD hysteresis loop would exist even in a symmetrical network with uniform demand. Therefore, large urban networks may have MFD hysteresis loops. In such cases, analysis of the effects of traffic-control strategies must consider the characteristics of such loops; the use of idealized, low-scattered MFD curves alone may compromise the accuracy of evaluation. However, traffic-control assessments that consider MFD hysteresis have not yet been performed. Moreover, the effects of traffic-control on the overall performance of a multi-modal network have been little-studied because of the complexity of individual mode, route, and departure time choices. Our objective was to close this literature gap. We explore the effect of MFD loop size on density spatial distribution and network performance. Specifically, we analyze these relationships for an interacting multi-modal network by simulating different traffic conditions for cars and buses using a multi-agent simulation framework (MATSim). Prior studies on MFD hysteresis are reviewed in Section 2. Section 3 illustrates our methodology and Section 4 our results. Finally, the principal conclusions are drawn in Section 5.

Nomenclature

Q_t	weighted average network flow at time t (veh/h).
K_t	weighted average network density at time t (veh/km).
$q_{i,t}$	flow of link i at time t.
$k_{i,t}$	density of link i at time t.
l_i	length of link i.
z	set of links in the network.
$\overline{K}_t$	average link density at time t.
σ_t	standard deviation of density at time t.
$\bar{\sigma}_{hys}$	average standard deviation of the density over a hysteresis loop (hys).
T_j	trip travel time of traveler j (min).
$\overline{TT}_{hys}$	average total passenger travel time over a hysteresis loop (hys).
DT_t	the set of travelers whose departure time is t.

2. Literature review

Geroliminis and Daganzo (2008) empirically observed an MFD in play in the Yokohama road network using data from loop detectors and GPS data from taxis. Later, several empirical studies (e.g., Geroliminis and Sun, 2011, Saberi and Mahmassani, 2012) and simulations (e.g., Ji et al., 2010, Gayah, et al., 2014) used MFDs to study urban networks and freeways. Many researchers (e.g., Knoop et al., 2012, Zheng et al., 2012, Keyvan-Ekbatani et al., 2013, Simoni et al., 2015, Zheng et al., 2016) assessed traffic-control strategies using MFDs and concluded that MFDs were useful when evaluating transportation network performance. However, some studies found that MFDs may contain hysteresis loops (multiple flows for a given density) (e.g., Buisson and Ladier, 2009, Mazloumian et al., 2010, Gayah and Daganzo, 2011, Daganzo et al., 2011). It was suggested that MFD hysteresis might develop when demand was not uniformly distributed or because surface streets, city centers, and suburban roads exhibited different characteristics. Gayah and Daganzo (2011) explored MFD hysteresis using a simplified two-bin network and found that hysteresis existed even when the network was symmetrical with uniform demand. Although MFD hysteresis may affect transportation network performance and density distribution evaluations, few studies are available in the literature. Using loop detector data for Portland, Saberi and Mahmassani (2012) studied the effects of spatial and temporal congestion and found that density heterogeneity among network links increased MFD scattering. Saberi and Mahmassani (2013) investigated MFD hysteresis in Chicago, Portland, and Irvine freeway networks using loop detector data, correlating the density distribution (the standard deviation of network occupancy during the recovery period) with the area of the hysteresis loop. However, no relationship of density to either loop width or height was apparent. Shi and Lin (2014) used loop detector data to investigate the MFD of an urban expressway network in Shanghai. The mean speed correlated directly with the hysteresis loop width but not the height (the capacity drop). Orfanou et al. (2012) used video data from the I-80 freeway in San Francisco to explore relationships between hysteresis loop shape and all of capacity drop, acceleration, and spacing. They classified drivers following other vehicles as aggressive or timid. A counter-clockwise hysteresis loop occurred when drivers were aggressive and a clockwise hysteresis loop when drivers were timid. Loop formation and duration were affected by driver spacing and acceleration, but not capacity drop. Recently, Muhlich et al. (2015) simulated various urban networks differing in terms of local street and arterial characteristics, using MFDs to compare traffic performance. The sizes and shapes of the hysteresis loops indicated that arterials strongly affected the density spatial distribution. Network performances were visually compared in terms of hysteresis loop width and height, but quantitative relationships were not explored.

In summary, the relationships between MFD hysteresis loop and traffic characteristics require further study. The relationship between the capacity drop and network conditions is not fully understood, and hysteresis loops in multi-modal networks have not been quantitated; these are the topics of this study.

3. Methodology

In our preliminary research, Hemdan et al. (2017) simulated various travel choices for a multi-modal network and used an MFD to compare them visually; quantitation was not attempted. Here, we sought relationships between loop height and width, and network density distribution (the standard deviation of link densities). We estimated MFDs for traffic conditions associated with various mode-share ratios on the Sioux Falls network, using a multi-agent transport simulation (MATSim). The extended Sioux Falls network used by Chakirov and Fourie (2014) was employed; this features urban roads and highways, with 334 links and 282 nodes. The bus network consists of five bus lines with 5-min headway operations. A total of 168,220 daily trips were simulated (56,904 workers traveling, and 27,206 persons performing secondary activities). Each person engaged in only one round trip per day (home–work–home or home–elsewhere–home). Work activity commenced at 8 a.m. and ended at 6 p.m., and typically lasted 9 h (latest work start: 9 a.m.); secondary trips were taken between 8 a.m. and 8 p.m. and were completed within 1 h.

Mode choice was expressed using a random utility model featuring an agent-based, stochastic user equilibrium (SUE). The MATSim was performed employing an integrated public transport simulation, in which buses share road space with cars and are affected by congestion. Integrated simulation of private and public transport based on a queuing model allows time-dependent calculation of travel times and evaluation of spillover effects. As shown in Table 1, we tested various supply characteristics and mode-choice combinations for considering a range of MFD loops. The simulation framework presented here enables mode choices for some individuals; some may choose to use a car, a bus, or to walk. We considered only two modes: cars and buses. We simulated a network featuring mode-choice re-planning; we fixed the marginal disutility for the bus mode and varied the marginal disutility for the car mode. Mode-choice re-planning probabilities were permitted for 10% of people. We performed the simulation for 1000 iterations. In each iteration, 10% of the agents were allowed for re-planning their mode, while all other agents chose an existing plan. After reaching a relaxed system state with (almost) constant average travel times and constant average realized utility from iteration to iteration, we simulated 100 more iterations without re-planning and considered the output of the last iteration to be in SUE and used its result for our analysis. The reliability of this method has been proved in many studies (e.g., Rieser, 2010, Grether, et al., 2009). Rieser (2010) validated these criteria by comparing simulation results with theoretical values for a simple hypothetical transit network based on the bottleneck model (Vickrey, 1969) and found that the analytical calculation and the simulation produce the same results. More details on MATSim and the travel choice mechanisms can be found in Balmer et al. (2006). We used MATSim outputs to calculate average network flows, average network densities, the standard deviations of density among the links, and the average passenger travel time, using the following equations:

$$Q_t = \frac{\sum_{i \in z} q_{i,t} l_i}{\sum_{i \in z} l_i} \tag{1}$$

$$K_t = \frac{\sum_{i \in z} k_{i,t} l_i}{\sum_{i \in z} l_i} \tag{2}$$

$$\sigma_t = \sqrt{\frac{\sum_{i \in z} \left(l_i (k_{i,t} - \bar{K}_t)^2\right)}{\sum_{i \in z} l_i}} \tag{3}$$

$$\bar{\sigma}_{hys} = \sqrt{\frac{\sum_{t \in hys} \sum_{i \in z} \left(l_i (k_{i,t} - \bar{K}_t)^2\right)}{\sum_{i \in z} l_i}} \tag{4}$$

$$TT_t = \sum_{j \in DT_t} T_j \tag{5}$$

$$\overline{TT}_{hys} = \frac{\sum_{t \in hys} \sum_{j \in DT_t} T_j}{\sum_{j \in DT_t} DT_t} \tag{6}$$

Table 1. The various network characteristics and mode-choice combinations (Sioux Falls network).

Scenario	Link type	Network characteristics						Mode-share ratio		
		No. of lanes		Free flow speed km/h		Flow capacity veh/h		Car %	Bus %	Walk%
		Urban	Highway	Urban	Highway	Urban	Highway			
Scenario 1	Urban	2	NA	50	NA	2000	NA	78%	19%	3%
Scenario 2	Urban	2	NA	50	NA	1500	NA	78%	19%	3%
Scenario 3	Urban	1	NA	50	NA	2000	NA	78%	19%	3%
Scenario 4	Urban & Highway	2	3	50	90	800:1000	1700:1900	58%	34%	8%
Scenario 5	Urban & Highway	2	3	50	90	800:1000	1700:1900	55%	36%	8%
Scenario 6	Urban & Highway	2	3	50	90	800:1000	1700:1900	52%	39%	9%

4. Results

We used Python to draw MFDs for different scenarios based on the MATSim outputs (Figure 1). We correlated loop dimensions with the density standard deviations and the average passenger travel time (a measure of network performance) using MFDs developed by Hemdan et al. (2017); these afford a wide range of mode-share ratios under various conditions (Figure 2). Following Saberi and Mahmassani (2013) and Shi and Lin (2014), we represented hysteresis loops in terms of width (the density difference), height (capacity drop), and area. After Xu et al. (2014), we divided the MFD loop into two portions, congestion onset and offset (associated with the maximum flow and loop start points). Xu et al. (2014) developed a method that automatically derived MFD hysteresis loops based on network flow-density data. The method requires identification of the loop transition points (the maximum flow, and the start and end points of the loop). The density distribution was more heterogeneous at the loop start point. Thus, we considered that examination of transition points might explain why the effect of capacity drop has not been discussed in the literature; this may have been present at some stage but was missed when examining overall loop intervals. Figure 3 shows our partitioning criterion and the transition points of the MFD hysteresis loop. Saberi and Mahmassani (2013) calculated the density standard deviation during the recovery period only; we calculate the values during both the loading and recovery periods and explore the relationships thereof with the sizes of the MFD hysteresis loops. Different relationships were found in terms of the average density standard deviation (for the recovery phase alone, and for the loading and recovery phases together), and the average passenger travel time. Table 2 shows the R^2 values.

In terms of whole-loop metrics, Table 2 shows that the density standard deviation is directly correlated with the loop area and width. Consideration of both the loading and recovery periods improved the correlations between the density standard deviation, and loop area and width (the R^2 values increase in the second row), perhaps because the loop is larger than that of Saberi and Mahmassani (2013). However, Wang (2016) empirically proved the existence of large loops. Consistent with Orfanou et al. (2012), Saberi and Mahmassani (2013), and Shi and Lin (2014), Table 2 shows that the density standard deviation is weakly correlated with MFD whole-loop height. The average passenger travel time is correlated with the whole-loop area and width, but only weakly with height. The overall loop area clearly correlates with both the density standard deviation and the average travel time, reflecting its correlation with density distribution and network performance. However, some important conclusions can be derived via MFD loop partitioning:

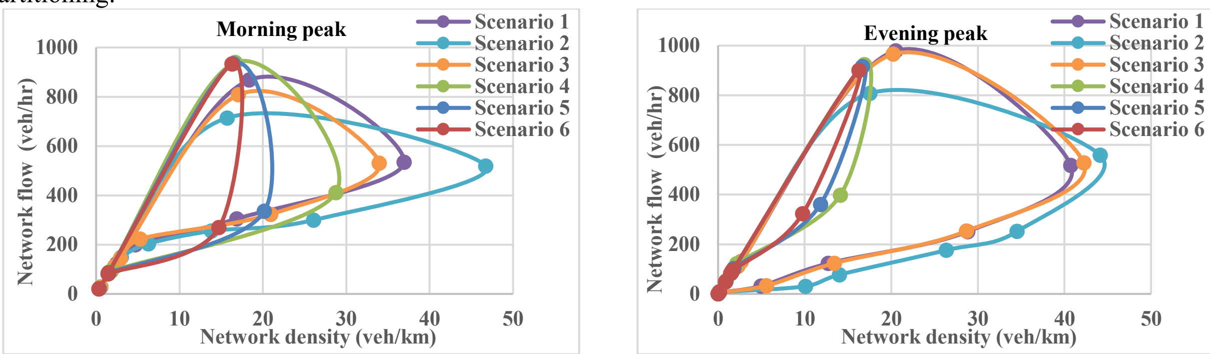

(a) (b)

Fig. 1. MFDs for different scenarios: (a) morning peak, (b) evening peak.

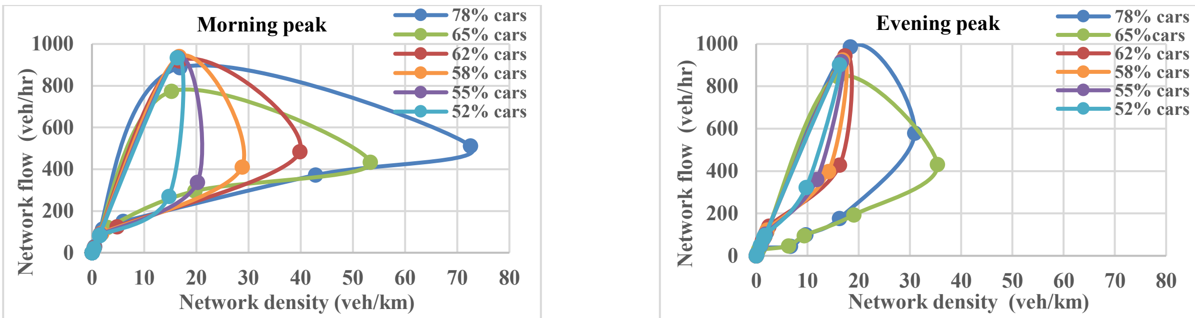

(a) (b)

Fig. 2. MFDs for different mode-share ratios: (a) morning peak, (b) evening peak (Hemdan et al., 2017).

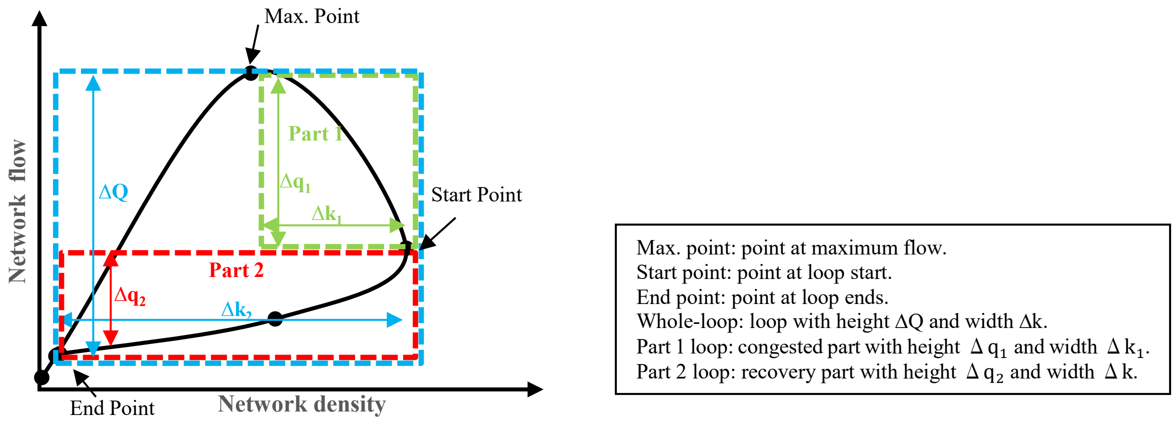

Fig. 3. Transition points on MFD loops.

Table 2. R^2 values for relationships between density standard deviations and loop metrics.

	Whole-loop			Part 1 loop			Part 2 loop		
	(ΔQ*Δk)	Δk	Δq	(Δq_1*Δk_1)	Δk_1	Δq_1	(Δq_2*Δk)	Δk	Δq_2
Average density standard deviation (calculated during recovery only)	0.762	0.634	0.046	0.554	0.570	–0.320	0.862	0.634	0.841
Average density standard deviation (calculated during both loading and recovery phases)	0.784	0.721	0.021	0.578	0.646	–0.390	0.902	0.721	0.857
Average passenger travel time	0.860	0.883	0.336	0.767	0.806	–0.701	0.888	0.883	0.510

- The correlations between the density standard deviation and the metrics (area, width, and height) of the Part 2 loop are stronger than those for the overall loop. Thus, the Part 2 loop alone represents the heterogeneity effect. The method developed by Xu et al. (2014) can be used to calculate directly the size of the Part 2 loop. Such information may suffice to describe the relationship between flow-density conditions and the spatial distribution of congestion; detailed traffic modeling is not required.
- The correlations between the density standard deviation and the heights of the Parts 1 and 2 loops (R^2 = 0.390 and 0.857 for $\Delta q1$ and $\Delta q2$, respectively) are stronger than the correlation with overall loop height (R^2 = 0.021). The same conclusion can be drawn for average passenger travel time. The correlations of the Part 1 and 2 loop heights with both density standard deviation and average passenger travel time are opposite in sign (Figures 4 and 5). This affects the relationship between the density standard deviation and the overall loop height (capacity drop), explaining the lack of correlations in the works of Orfanou et al. (2012), Saberi and Mahmassani (2013) and Shi and Lin (2014) . Two explanations are advanced:
  1) $\Delta q1$ is the capacity drop occurring while demand remained high (the network was loading) and is associated with the inability of the network to sustain the maximum capacity for a long time (Saberi and Mahmassani, 2013). During congestion, more loading triggers less heterogeneity because all links are congested; this decreases network flow and, consequently, increases $\Delta q1$. Thus, $\Delta q1$ increases with a decrease in the density standard deviation.
  2) $\Delta q2$ occurs during recovery. As congestion dissipates, the densities of many links decrease; however, some links are still congested, creating a higher density standard deviation. The flow on most links falls (because of either congestion or low link occupancy) and, consequently, $\Delta q2$ increases. Thus, the larger the $\Delta q2$, the more heterogeneous the congestion distribution during recovery.

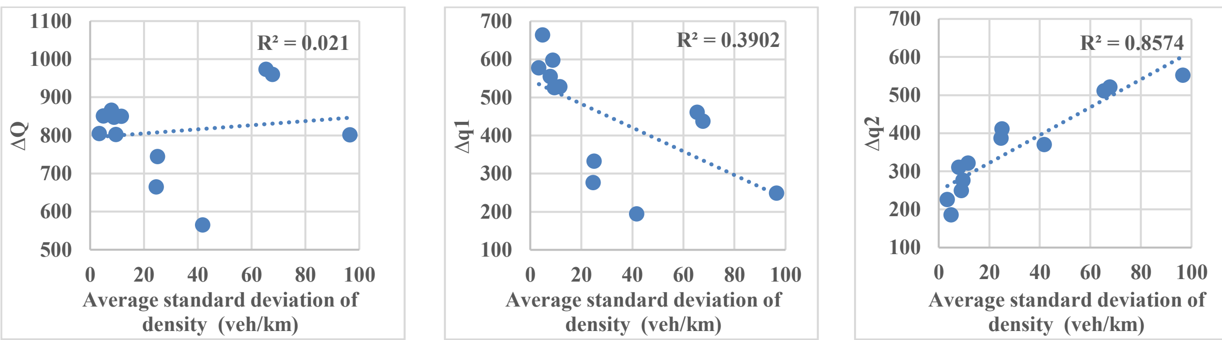

(a) (b) (c)

Fig. 4. Relationships between density standard deviations and: (a) the height of the overall loop (ΔQ), (b) the height of the Part 1 loop ($\Delta q1$), and (c) the height of the Part 2 loop ($\Delta q2$).

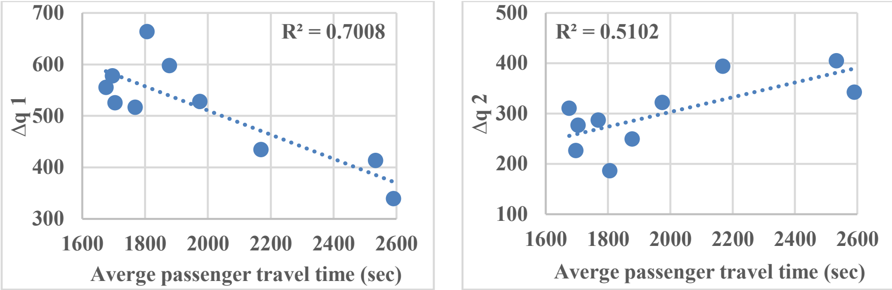

(a) (b)

Fig. 5. Relationships between average passenger travel time and the height of the: (a) Part 1 loop (Δq1) and, (b) Part 2 loop (Δq2).

It is clear from Table 2 and Figures 4 and 5 that the R^2 value for the correlation of density standard deviation with the height of the Part 2 loop is higher than that for the height of the Part 1 loop. Also, the R^2 value for the average passenger travel time correlation with the height of the Part 1 loop is higher than that with the height of the Part 2 loop. Thus, network performance negatively affects capacity drop during network loading, and the inhomogeneous spatial distribution of congestion increases flow reduction during network unloading as congestion dissipates. Capacity drop in the Part 1 loop is attributable to network loading, although maximum flow cannot be sustained for long. More loading decreases network flow (Δq1 increases). Δq2 develops during congestion dissipation as some link densities decrease and some remain congested, creating a higher density standard deviation accompanied by a Δq2 increase.

5. Summary and conclusion

It is difficult to draw low-scattered MFDs for real-world city-scale networks (at the same average network density, average network flow as congestion builds is greater than during congestion dissipation); hysteresis loops thus develop. The relationships between these loop sizes and network-wide traffic conditions are of great practical importance when comparing traffic-control strategies. We explored relationships between the size of the MFD hysteresis loop, and the spatial density distributions and network performance. We utilized a multi-agent transport simulation tool to develop different traffic conditions on the Sioux Falls network, and we programmed various mode-share ratios (cars and buses). Mode choice was expressed based on a random utility model featuring an agent-based, stochastic user equilibrium. We approximated MFD hysteresis loop areas as the products of width and height (Saberi and Mahmassani, 2013, Shi and Lin, 2014). We correlated loop dimensions with density standard deviations (representing special density distributions) and average passenger travel times (representing network performances). In addition, we partitioned the loop area into two parts (the congestion-building and -dissipation periods). Then, we correlated the average density standard deviations and passenger travel times with the sizes of the overall loop and its parts. We conclude that calculating average density standard deviations during both the loading and recovery periods improves the correlation strengths. In particular, when the MFD loop was partitioned into upper and lower parts (the congestion-building and -dissipation periods, respectively), the correlation between the density standard deviation and the lower loop was stronger than that with the overall loop. Thus, the lower loop alone represents the heterogeneity effect. Such heterogeneous density distribution increases flow reduction during network unloading as congestion dissipates. We also found that the correlations between the density standard deviations and the heights of both the Part 1 and 2 loops were stronger than the correlation with overall loop height, because the two loop heights exerted opposite effects on the density standard deviation, explaining why no relationship between capacity drop and congestion inhomogeneity was found in previous research (Saberi and Mahmassani, 2013, Shi and Lin, 2014, Orfanou et al., 2012). Also, the average passenger travel time was inversely correlated with the height of the upper part of the loop. Thus, network performance inversely affects the capacity drop when the network is loading.

We found that MFD hysteresis could be used to compare traffic-control strategies simply, facilitating appropriate decision-making. Although our simulations are promising, empirical real data for a multi-modal network require evaluation. Practical application of our method requires detailed information on vehicle- and people-flow counts, vehicle occupancies, and origin-destination matrices.

References

Balmer, M., Axhausen, K., Nagel, K., 2006. Agent-Based Demand-Modeling Framework for Large-Scale Microsimulations. Transportation Research Record: Journal of the Transportation Research Board 1985, 125–134.

Buisson, C., Ladier, C., 2009. Exploring the Impact of Homogeneity of Traffic Measurements on the Existence of Macroscopic Fundamental Diagrams. Transportation Research Record: Journal of the Transportation Research Board 2124, 127–136.

Chakirov, A., Fourie, P.J., 2014. Enriched Sioux Falls Scenario with Dynamic and Disaggregate Demand. Technical Report. Future Cities Laboratory, Singapore ETH Centre (SEC).

Daganzo, C. F., Gayah, V. V., Gonzales, E. J., 2011. Macroscopic Relations of Urban Traffic Variables: Bifurcations, Multivaluedness and Instability. Transportation Research Part B: Methodological 45.1, 278–288.

Gayah, V. V., Daganzo, C. F., 2011. Clockwise Hysteresis Loops in the Macroscopic Fundamental Diagram: An Effect of Network Instability. Transportation Research Part B: Methodological 45.4, 643–655.

Gayah, V. V., Gao, X., Nagle, A. S., 2014. On the Impacts of Locally Adaptive Signal Control on Urban Network Stability and the Macroscopic Fundamental Diagram. Transportation Research Part B: Methodological 70, 255–268.

Geroliminis, N., Daganzo, C. F., 2008. Existence of Urban-Scale Macroscopic Fundamental Diagrams: Some Experimental Findings. Transportation Research Part B: Methodological 42.9, 759–770.

Geroliminis, N., Sun, J., 2011. Properties of a Well-Defined Macroscopic Fundamental Diagram for Urban Traffic. Transportation Research Part B: Methodological 45.3, 605–617.

Grether, D., Chen, Y., Rieser, M., Nagel, K., 2009. Effects of a Simple Mode Choice Model in a Large-Scale Agent-Based Transport Simulation. In Advances in Spatial Science, Complexity and Spatial Networks. Springer Berlin Heidelberg, 167–186.

Hemdan, S., Wahaballa, A. M., Kurauchi, F., 2017. Evaluating Travel Choices Effect on Multimodal Network Performance Using Vehicle and Passenger Macroscopic Fundamental Diagrams. Journal of the Eastern Asia Society for Transportation Studies 12, 1710–1727.

Ji, Y., Daamen, W., Hoogendoorn, S., Hoogendoorn-Lanser, S., Qian, X., 2010. Investigating the Shape of the Macroscopic Fundamental Diagram Using Simulation Data. Transportation Research Record: Journal of the Transportation Research Board 2161, 40–48.

Keyvan-Ekbatani, M., Papageorgiou, M., Papamichail, I., 2013. Urban Congestion Gating Control Based on Reduced Operational Network Fundamental Diagrams. Transportation Research Part C: Emerging Technologies 33, 74–87.

Knoop, V., Hoogendoorn, S., Van Lint, J., 2012. Routing Strategies Based on Macroscopic Fundamental Diagram. Transportation Research Record: Journal of the Transportation Research Board 2315.1, 1–10.

Mazloumian, A., Geroliminis, N., Helbing, D., 2010. The Spatial Variability of Vehicle Densities as Determinant of Urban Network Capacity. Philosophical Transactions of the Royal Society A: Mathematical, Physical and Engineering Sciences 368.1928, 4627–4647.

Muhlich, N., Gayah, V. V, Menendez, M., 2015. An Examination of MFD Hysteresis Patterns for Hierarchical Urban Street Networks Using Micro-Simulation. Transportation Research Record: Journal of the Transportation Research Board 2491, 117–126.

Orfanou, F., Vlahogianni, E., Karlaftis, M. (2012) Identifying Features of Traffic Hysteresis on Freeways. Transportation Research Board 91st Annual Meeting, Washington, DC, paper #12-1587.

Rieser, M.,2010. Adding Transit to an Agent-Based Transportation Simulation. PhD dissertation, Swiss Federal Institute of Technology.

Saberi, M., Mahmassani, H.S., 2012. Exploring Properties of Networkwide Flow-Density Relations in a Freeway Network. Transportation Research Record: Journal of Transportation Research Board 2315, 153–163.

Saberi, M., Mahmassani, H.S., 2013. Empirical Characterization and Interpretation of Hysteresis and Capacity Drop Phenomena in Freeway Networks. Transportation Research Record: Journal of the Transportation Research Board 2391, 44–55.

Shi, X. Lin, H., 2014. Exploring the Characteristics of Hysteresis Phenomena of Macroscopic Fundamental Diagram for Urban Expressway Network: The Case of Shanghai. Transportation Research Board 93rd Annual Meeting, Washington, DC, paper #14-2060.

Simoni, M. D., Pel, A.J., Waraich, R.A., Hoogendoorn, S.P., 2015. Marginal Cost Congestion Pricing Based on the Network Fundamental Diagram. Transportation Research Part C: Emerging Technologies 56, 221–238.

Vickrey, W., 1969. Congestion Theory and Transport Investment. American Economic Review, 59.2, 251-260.

Wang, P., 2016. Exploring the Features of Macroscopic Fundamental Diagram and Its Formation Mechanism Based on Long-Term Detectors Data: Empirical Studies on Urban Road Networks in Japan. PhD dissertation, Tohoku University.

Xu, Z., Jin, P.J., Zhang, J., Ran, B., 2014. An Automatic Calculation Method of Identifying the Hysteresis Loop Characteristics in Macroscopic Fundamental Diagram. Transportation Research Board 93rd Annual Meeting, Washington, DC, paper #14-2305.

Zheng, N., Rérat, G., Geroliminis, N., 2016. Time-Dependent Area-Based Pricing for Multimodal Systems with Heterogeneous Users in an Agent-Based Environment. Transportation Research Part C: Emerging Technologies 62, 133–148.

Zheng, N., Waraich, R.A., Axhausen, K.W., Geroliminis, N., 2012. A Dynamic Cordon Pricing Scheme Combining the Macroscopic Fundamental Diagram and an Agent-Based Traffic Model. Transportation Research Part A: Policy and Practice 46.8, 1291–1303.